D. I. Morís, J. de Moura, J. Novo and M. Ortega, "Cycle Generative Adversarial Network Approaches to Produce Novel Portable Chest X-Rays Images for Covid-19 Diagnosis," ICASSP 2021 - 2021 IEEE International Conference on Acoustics, Speech and Signal Processing (ICASSP), Toronto, ON, Canada, 2021, pp. 1060-1064, doi: 10.1109/ICASSP39728.2021.9414031

Link to published version: https://doi.org/10.1109/ICASSP39728.2021.9414031

CYCLE GENERATIVE ADVERSARIAL NETWORK APPROACHES TO PRODUCE NOVEL PORTABLE CHEST X-RAYS IMAGES FOR COVID-19 DIAGNOSIS

Daniel I. Morís[⋆†] *Joaquim de Moura*[⋆†] *Jorge Novo*[⋆†] *Marcos Ortega*[⋆†]

[⋆] Centro de investigación CITIC, Universidade da Coruña, 15071, A Coruña, Spain
[†] Grupo VARPA, Instituto de Investigación Biomédica de A Coruña (INIBIC), Universidade da Coruña, 15006, A Coruña, Spain

ABSTRACT

Coronavirus Disease 2019 (COVID-19), declared a global pandemic by the World Health Organization, mainly affects the pulmonary tissues, playing chest X-ray images an important role for its screening and early detection. In this context, portable X-ray devices are widely used, representing an alternative to fixed devices in order to reduce risks of cross-contamination. However, they provide lower quality and detailed images in terms of spatial resolution and contrast. In this work, given the low availability of images of this recent disease, we present new approaches to artificially increase the dimensionality of portable chest X-ray datasets for COVID-19 diagnosis. Hence, we combined 3 complementary CycleGAN architectures to perform a simultaneous oversampling using an unsupervised strategy and without the necessity of paired data. Despite the poor quality of the portable X-ray images, we provide an overall accuracy of 92.50% in a COVID-19 screening context, proving their suitability for COVID-19 diagnostic tasks.

***Index Terms*—** COVID-19, Portable chest X-ray images, Oversampling, CycleGAN, Deep Learning

1. INTRODUCTION

The novel coronavirus SARS-CoV-2 appeared in Wuhan, Hubei province (China) at the end of 2019 and was rapidly spread worldwide. It causes a respiratory infection known as Coronavirus disease 2019 (COVID-19) that was declared as a global pandemic by the World Health Organization (WHO) [1]. The most common symptoms of COVID-19 are fever, coughing, pneumonia or respiratory distress syndrome, making the disease difficult to distinguish from other common infections like pneumonia or influenza-like viruses [2].

During the last decades, chest X-ray images have been widely used as a method for the clinical diagnosis of relevant pulmonary issues and diseases like fibrosis, pneumonia, pleural thickening or lung nodules, among others [3]. In the context of the global pandemic caused by the COVID-19 disease, radiologists are asked to prioritize chest X-ray images of patients with clinical-epidemiological suspected COVID-19 infection over any other imaging evaluations.

Given the relevance of this topic, several works have been aimed at solving the problem of automatic screening for COVID-19 using the chest X-ray images. In this sense, deep learning has shown a significant performance, providing satisfactory results [4, 5, 6, 7].

Typically, the availability of sufficient images is crucial for the development of accurate CAD systems. Thus, few studies specifically addressed the paradigm of oversampling over chest X-ray datasets. As reference, Malygina *et al.* [8] proposed a methodology for the oversampling of X-ray images using a Cycle Generative Adversarial Network (CycleGAN) in the analysis of pneumonia.

Given the recent apparition of the COVID-19 disease, the image availability is still reduced. In that context, at the moment, only Zebin *et al.* [9] used a CycleGAN to generate new images, considering only the minority COVID-19 class. Therefore, this work partially addresses the problem, without considering all the classes for oversampling, which may bias the final learning process. In addition, the authors used the COVID-19 Image Data Collection [10], where the X-ray images, mostly from fixed capture devices with good quality and detail, were extracted from online publications, websites, or directly from the PDF files using cropping tools and, therefore, without any reference to the type of X-ray device used. In this line, the American College of Radiology (ACR) recommends to use portable chest X-ray machinery [11], which is critical to minimize the risks of COVID-19 transmission [12]. However, portable X-ray devices provide lower quality images in terms of spatial resolution and contrast, providing

This research was funded by Instituto de Salud Carlos III, Government of Spain, DTS18/00136 research project; Ministerio de Ciencia e Innovación y Universidades, Government of Spain, RTI2018-095894-B-I00 research project; Ministerio de Ciencia e Innovación, Government of Spain through the research project with reference PID2019-108435RB-I00; Consellería de Cultura, Educación e Universidade, Xunta de Galicia, Grupos de Referencia Competitiva, grant ref. ED431C 2020/24; Axencia Galega de Innovación (GAIN), Xunta de Galicia, grant ref. IN845D 2020/38; CITIC, Centro de Investigación de Galicia ref. ED431G 2019/01, receives financial support from Consellería de Educación, Universidade e Formación Profesional, Xunta de Galicia.

lower details for the diagnostic process. Therefore, an image-based computational analysis is more challenging compared to images from fixed X-ray devices that are of better quality.

In this work, we propose a novel fully automatic methodology for artificially increasing the dimensionality of the chest X-ray dataset, using an unsupervised strategy and without the necessity of using paired data. To achieve this, we combined 3 complementary CycleGAN architectures to perform a complete oversampling task, simultaneously considering the different combinations among healthy, pathological and genuine COVID-19 cases. To validate our proposal, exhaustive experiments were performed using a portable X-ray dataset that was obtained from a real COVID-19 diagnostic context. Despite the poor quality, portable X-ray images are now frequently used in healthcare services, minimizing infection control problems and, therefore, the risk of cross-contamination. To the best of our knowledge, this proposal represents the only study specifically designed for the oversampling and analysis of COVID-19 in chest X-ray images acquired by means of portable devices, in combination with healthy patients and other pulmonary diseases.

2. MATERIALS AND METHODS

The proposed methodology is divided into 2 main stages, as illustrated in Fig. 1. Firstly, a set of generated X-ray images is obtained, taking advantage of 3 complementary CycleGAN architectures in order to perform a simultaneous oversampling using an unsupervised approach (Section 2.2) of all the possible situations: healthy patients, pulmonary pathological patients and genuine COVID-19 patients. After that, the system provides a computational approach for the analysis of the degree of separability between chest X-ray images of the different possible scenarios of pulmonary diseases (Section 2.3).

2.1. Dataset

All the X-ray images were provided by the Radiology Service of the Complexo Hospitalario Universitario A Coruña (CHUAC). They were obtained from portable devices from a real COVID-19 screening context. These images, despite that provide less quality and details, are frequently used at the moment in the healthcare services in this diagnostic scenario given the flexibility and versatility of the capture devices. Specifically, the particular used capture models were Agfa dr100E GE and Optima Rx200. This dataset, designed specifically for this study, consists of 600 chest X-ray images from 600 patients divided into 200 healthy cases, *i.e.* without pleural or pulmonary diseases (without considering cardiology or hepatic diseases), 200 pathology cases, *i.e.* patients diagnosed with pulmonary diseases that can be present symptoms similar to COVID-19 and 200 genuine COVID-19 cases.

2.2. Computational approaches for data augmentation

To obtain the augmented dataset, the oversampling paradigm is divided into 3 different scenarios considering the combinations among healthy, pathological and COVID-19 cases.

Healthy vs Pathological. In this case, the set of healthy images is considered alongside the pathological images. From this analysis, two different pathways are followed. The first one translates the images from healthy to pathological. Regarding this idea, the system adds pathological patterns that belong to diseases others than COVID-19. On the other hand, the second pathway converts the images from the pathological scenario to a healthy environment.

Healthy vs COVID-19. Chest X-ray images labeled as healthy are translated to a COVID-19 environment. Similarly, two pathways are followed. The first one converts healthy images to COVID-19, presumably adding pathological patterns compatible with COVID-19. In the second pathway the network should remove COVID-19 pathological patterns from the images, generating synthetic healthy images.

Pathological vs COVID-19. Similarly, in the first pathway, images labeled as pathological are converted to a COVID-19 scenario. The method should remove pathological patterns from the original image, then adding structures related with the COVID-19 disease. In the second pathway, the same idea is considered but in the opposite direction.

Network architecture and training details. The whole amount of images is used for training the CycleGAN [13] architecture. Hence, we adopted a ResNet-based generator with 9 residual blocks as discriminating network. All the approaches of this stage have the same parameter set. Every model is trained using the Adam algorithm from scratch during 250 epochs with a mini-batch size of 1 and a constant learning rate of $\alpha = 0.0002$ during the whole process.

2.3. Computational approach for screening tasks

For the second stage, we designed a computational approach for the analysis of the degree of separability between chest X-ray images and the suitability of the generated samples. On one hand, we analyze the separability between the images generated by the oversampling process. Also, we analyzed the COVID-19 screening using the new oversampled dataset.

Network architecture and training details. A Dense Convolutional Network Architecture (DenseNet) [14] was used, in this state, to test their potential in the proposed approaches. The training details of this experiment are the same used in [15], given their adequate results for this issue. Thus, the input dataset was randomly partitioned in three sets with the 60% of the images for training, 20% for validation and the remaining 20% for testing purposes. In addition, the weights from a model pretrained on the ImageNet dataset was used for the network initialization. In particular, this model was trained using cross-entropy as loss function. The network weights optimization was performed using the algorithm of

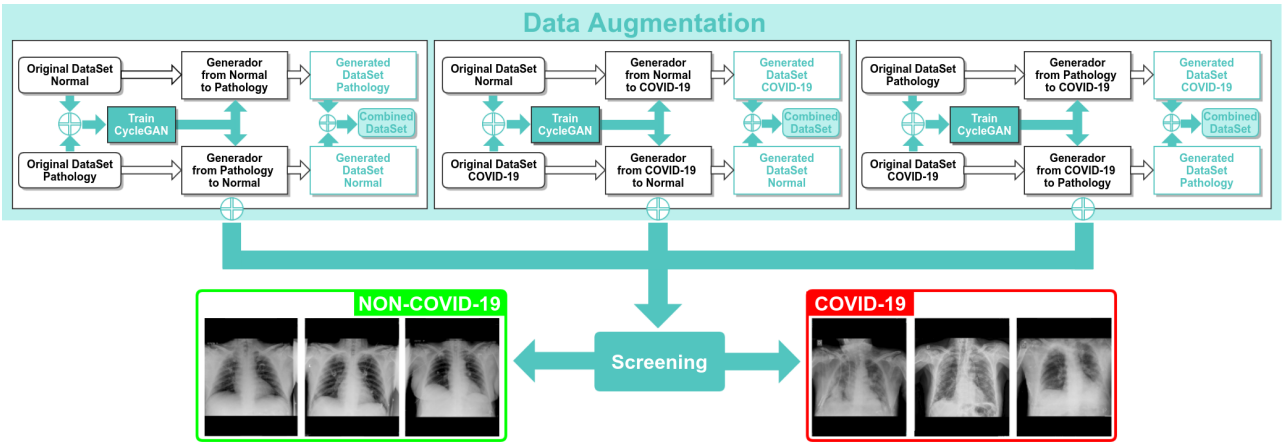

Fig. 1: A general overview of the proposed paradigm.

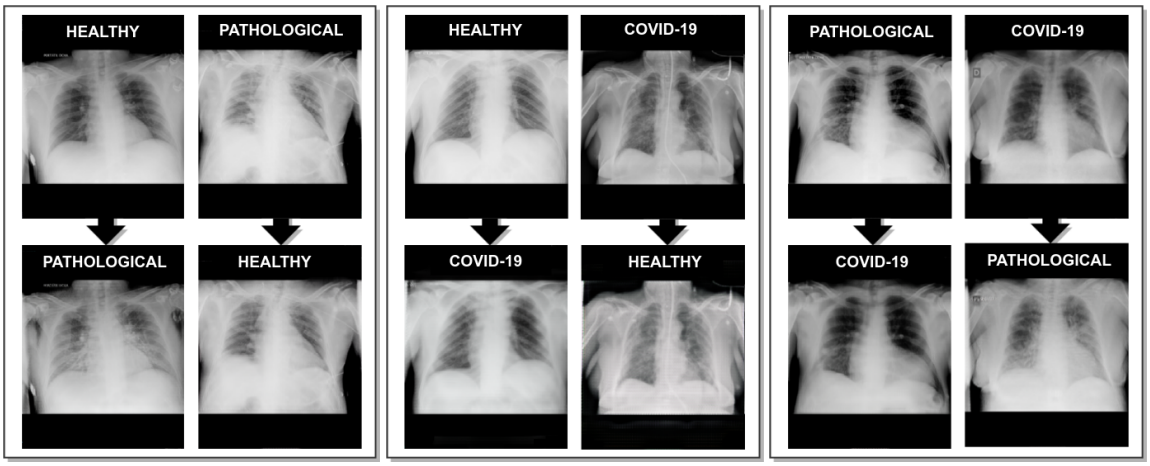

Fig. 2: Examples of generated chest X-ray images from the complete oversampling methodology. 1^{st} block, healthy vs Pathological scenario. 2^{nd} block, Healthy vs COVID-19 scenario. 3^{rd} Pathological vs COVID-19 scenario.

Stochastic Gradient Descent (SGD) with a constant learning rate with a value of $\alpha = 0.01$. In the same way, the value of mini-batch size was fixed to 4 and a first-order momentum of 0.9 was considered. With respect to the number of repetitions, this process was performed 5 times.

2.4. Evaluation

The performance of these proposed approaches was evaluated making a comparison between the actual annotations made in the original dataset against the outputs predicted by the network. Thus, considering the values of True Positives (TP), True Negatives (TN), False Positives (FP) and False Negatives (FN), several performance metrics commonly used were considered: precision, recall, F1-Score and accuracy.

3. EXPERIMENTAL RESULTS

In this work, 4 representative experiments were conducted. The first 3 were used to validate the degree of separability among the generated images obtained from the oversampling process and their genuine utility. Next, a fourth experiment was performed to distinguish between cases of patients with COVID-19 from other similar respiratory diseases or even healthy patients. Fig. 2 shows some representative examples of the generated images obtained from the CycleGAN oversampling approaches that illustrate the remarkable and well-synthesized differences in the pulmonary regions.

1^{st} experiment: analysis of the separability of healthy and pathological generated examples. In this first case, we designed an experiment to evaluate the capability of the system to convert images from healthy to pathological and vice versa. To do so, we consider the set of 200 healthy generated images alongside the set of 200 pathological generated images. The method achieved a mean accuracy of

0.9641 ± 0.0326 for training, 0.9100 ± 0.0533 for validation and a global accuracy of 0.9375 in terms of test (Table 1).

Table 1: Performance at the test stage for the separability between healthy and pathological generated examples.

Cases	Precision	Recall	F1-Score
Healthy	0.92	0.95	0.94
Pathological	0.95	0.93	0.94

2nd experiment: analysis of the separability of healthy and COVID-19 generated examples. In this second experiment, we proved the system capability of converting images from a healthy environment to a COVID-19 scenario and vice versa. To do so, we considered the 200 healthy generated images set alongside the 200 generated images with specific COVID-19 symptomatology. After 5 repetitions, the model achieved a mean train accuracy of 0.8970 ± 0.0981 for training, 0.8512 ± 0.0753 for validation and a global accuracy of 0.8687 in terms of testing (Table 2).

Table 2: Performance at the test stage for the separability between healthy and COVID-19 generated examples.

Cases	Precision	Recall	F1-Score
Healthy	0.84	0.90	0.87
COVID-19	0.90	0.84	0.87

3rd experiment: analysis of the separability of pathological and COVID-19 generated examples. In this approach, we proved the system ability to convert images from pathological to COVID-19 and vice versa. To do that, the whole set of 200 pathological generated images is used alongside the set of 200 COVID-19 generated examples. After 5 iterations the model obtained a mean accuracy of 0.9050 ± 0.1336 for training, 0.8587 ± 0.1333 for validation and a global accuracy of 0.9375 in terms of testing (Table 3).

Table 3: Performance at the test stage for the separability between pathological and COVID-19 generated examples.

Cases	Precision	Recall	F1-Score
Pathological	0.91	0.98	0.94
COVID-19	0.97	0.90	0.93

4th experiment: analysis of the COVID-19 screening using the original dataset with oversampling. In this last experiment, we designed a scenario to evaluate the degree of separability between cases of patients with COVID-19 from other similar respiratory diseases and even healthy patients. To do so, this approach considers both the original dataset (600 images) and the new generated dataset (1,200 images). In this case, we use a proportion of $\frac{2}{3}$ and $\frac{1}{3}$ between negative and positive classes, respectively. After 5 repetitions, the model achieved a mean accuracy of 0.9700 ± 0.0276 for training, 0.9050 ± 0.0315 for validation and a global accuracy of 0.9250 in terms of testing. Additionally, Fig. 3 shows the performance of the model in testing, showing a 0.9328 correct classification ratio for the Healthy/Pathological scenario whereas a 0.9098 ratio for the COVID-19 examples.

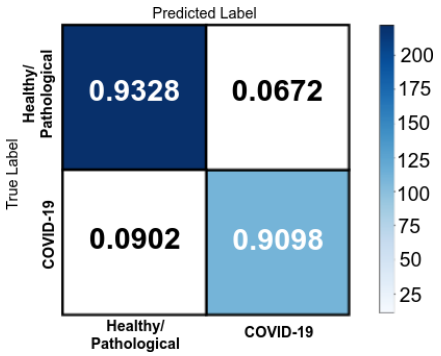

Fig. 3: Confusion matrix results for the 4th experiment on the test set with the ratios of correct classification and misclassification for the COVID-19 screening.

4. CONCLUSION

This work presents novel and fully automatic approaches specifically designed to artificially increase the size of the chest X-ray dataset used for COVID-19 diagnosis. The dataset specifically designed for this work has been provided by the Radiology Service of the Complexo Hospitalario Universitario A Coruña (CHUAC). All images were obtained from portable devices from a real COVID-19 diagnostic scenario. Due to their poor quality and details, portable X-ray images represent a significant challenge for the automatic diagnosis of COVID-19. In this complex scenario, 3 complementary CycleGAN architectures were used simultaneously to perform a complete oversampling of all the considered classes (healthy, pulmonary pathological and COVID-19), avoiding biases in the classification process. After that, the system provides a computational approach for the analysis of the degree of separability between chest X-ray images of the different possible scenarios of pulmonary diseases. Several experiments were conducted to prove that the proposal is able to translate portable X-ray images between different scenarios, generating a set of synthetic images with a suitable separability. In the same way, the obtained results show the robustness of the proposal in the screening of COVID-19, obtaining a high ratio of correct classifications for both the Healthy/Pathological and the specific COVID-19 cases.

5. REFERENCES

[1] Casey A Pollard, Michael P Morran, and Andrea L Nestor-Kalinoski, "The COVID-19 Pandemic: A Global Health Crisis," *Physiological Genomics*, 2020.

[2] S. Zayet, N. J. Kadiane-Oussou, Q. Lepiller, H. Zahra, P. Royes, L. Toko, V. Gendrin, and T. Klopfenstein, "Clinical features of COVID-19 and influenza: a comparative study on Nord Franche-Comte cluster," *Microbes and Infection*, 2020.

[3] S. Xu, H. Wu, and R. Bie, "CXNet-m1: Anomaly Detection on Chest X-Rays With Image-Based Deep Learning," *IEEE Access*, vol. 7, pp. 4466–4477, 2019.

[4] I. Apostolopoulos and M. Tzani, "Covid-19: Automatic detection from X-Ray images utilizing Transfer Learning with Convolutional Neural Networks," *Australasian physical & engineering sciences in medicine / supported by the Australasian College of Physical Scientists in Medicine and the Australasian Association of Physical Sciences in Medicine*, vol. 43, 2020.

[5] J. de Moura, J. Novo, and M. Ortega, "Fully automatic deep convolutional approaches for the analysis of Covid-19 using chest X-ray images," *medRxiv*, 2020.

[6] Lin Li, Lixin Qin, Zeguo Xu, Youbing Yin, Xin Wang, Bin Kong, Junjie Bai, Yi Lu, Zhenghan Fang, Qi Song, et al., "Artificial intelligence distinguishes COVID-19 from community acquired pneumonia on chest CT," *Radiology*, 2020.

[7] Shervin Minaee, Rahele Kafieh, Milan Sonka, Shakib Yazdani, and Ghazaleh Jamalipour Soufi, "Deep-covid: Predicting covid-19 from chest x-ray images using deep transfer learning," *arXiv preprint arXiv:2004.09363*, 2020.

[8] Tatiana Malygina, Elena Ericheva, and Ivan Drokin, "GANs' N Lungs: improving pneumonia prediction," *arXiv preprint arXiv:1908.00433*, 2019.

[9] Tahmina Zebin and Shahadate Rezvy, "COVID-19 detection and disease progression visualization: Deep learning on chest X-rays for classification and coarse localization," *Applied Intelligence*, pp. 1–12, 2020.

[10] Joseph Paul Cohen, Paul Morrison, Lan Dao, Karsten Roth, Tim Q Duong, and Marzyeh Ghassemi, "Covid-19 image data collection: Prospective predictions are the future," *arXiv preprint arXiv:2006.11988*, 2020.

[11] Soheil Kooraki, Melina Hosseiny, Lee Myers, and Ali Gholamrezanezhad, "Coronavirus (COVID-19) outbreak: what the department of radiology should know," *Journal of the American college of radiology*, 2020.

[12] Canadian Agency for Drugs, Technologies in Health, et al., "Portable versus Fixed X-ray Equipment: A Review of the Clinical Effectiveness, Cost-effectiveness, and Guidelines," *Rapid Response Report*, 2016.

[13] Jun-Yan Zhu, Taesung Park, Phillip Isola, and Alexei A Efros, "Unpaired image-to-image translation using cycle-consistent adversarial networks," in *Proceedings of the IEEE international conference on computer vision*, 2017, pp. 2223–2232.

[14] Gao Huang, Shichen Liu, Laurens Van der Maaten, and Kilian Q Weinberger, "Condensenet: An efficient densenet using learned group convolutions," in *Proceedings of the IEEE conference on computer vision and pattern recognition*, 2018, pp. 2752–2761.

[15] J. de Moura, L. Ramos, P. Vidal, M. Cruz, L. Abelairas, E. Castro, J. Novo, and M. Ortega, "Deep convolutional approaches for the analysis of Covid-19 using chest X-Ray images from portable devices," *medRxiv*, 2020.